Received: March 27, 2023. Revised: April 20, 2023.

INASS

International Journal of
Intelligent Engineering & Systems

http://www.inass.org/

Advanced Nonlinear Robust Approach for Controlling COVID-19 System Based on Vaccination Campaign

Ali H. Mhmood[1]* Hazem I. Ali[2] Amer B. Rakan[1] Mohammed R. Subhi[1] Yaseen Kh. Yaseen[1] Hameed A. Mohammed[1]

[1]*Petroleum Systems Control Engineering Department, College of Petroleum Processes Engineering, Tikrit University, Tikrit, Iraq*
[2]*Control and Systems Engineering Department, University of Technology-Iraq, Baghdad, Iraq*
* Corresponding author's Email: ali.h.mhmood@tu.edu.iq

Abstract: This study proposes a new approach for controlling COVID-19 through vaccination, where an adequately descriptive mathematical model is created for COVID-19 using the susceptible exposed infectious recovered (SEIR) model of epidemic diseases. The presented control approach is synthesized using a combination of feedback linearization and H_∞ control, and incorporates model reference control to achieve optimal time responses with the aid of the black hole optimization (BHO) algorithm. The effectiveness of the designed control law is evaluated using data from the lombardy region of Italy. The results of the simulation show that the proposed control approach is able to effectively control the COVID-19 outbreak by accurately implementing the desirable vaccination, while effectively addressing nonlinearity and uncertainty in the COVID-19 system with a desirable control action. The control method has achieved the required immunity of 6.6 million individuals after approximately 25 days with a transmission rate reduced to zero in a short time, and a vaccination rate of 170 thousand people per day.

Keywords: COVID-19, SEIR epidemic model, Vaccination, Nonlinear robust control, Model reference control, Black hole algorithm.

1. Introduction

The coronavirus disease (COVID-19) pandemic was originally reported in Wuhan, China, in late 2019, and has subsequently expanded worldwide. The disease causal organism has been recognized as the severe acute respiratory syndrome coronavirus 2 (SARS-CoV-2). The virus has the capability to transmit efficiently in population-dense settings and congregate environments, where individuals tend to congregate for extended periods of time [1]. Hence, the virus has rapidly disseminated across the globe, resulting in an epidemic crisis and exerting a negative influence on human social activities [2].

Prior to the development of vaccines, various public health strategies like mitigation, suppression, and herd immunity have been discussed as means of controlling COVID-19 [3-5]. These strategies have been implemented in various countries, with varying levels of efficacy dependent on the population's adherence to the prescribed policies. However, these measures are considered as temporary solutions to slow the progression of the outbreak until vaccines are developed. Lately, numerous vaccines including AstraZeneca-Oxford, Sinopharm, Moderna, and Pfizer-BioNTech have been produced and approved for use in several countries. These vaccines were demonstrated to be effective in avoiding COVID-19-related infection [6]. To efficiently manage the vaccination, governments have adopted automation systems that help in administering and monitoring the vaccination plan. In addition, several vaccination strategies have been studied in the literature [7-9] to combat the COVID-19 outbreak. For all vaccines, research studies indicate that the primary objective of vaccination is to reduce the transmission rate of the virus by increasing the immunity of individuals through vaccination and reducing the number of

susceptible individuals in the total population.

Control engineering has played an important role in the investigation of the COVID-19 communicable virus, providing a variety of mathematical models to analytically characterize the conduct of the COVID-19 system based on epidemic modelling, and many effective tactics to tackle it [10]. Various control methods were developed in the field, such as robust sliding mode control [11], Lyapunov analysis-based nonlinear robust control [12], robust optimal model predictive feedback control [13], state estimation-based nonlinear robust control [14], and nonlinear adaptive control [15]. The previous control methods primarily focused on the mitigation and suppression measures and assumed constant parameter values during the study period, despite the fact that these values may vary in reality.

Previous works have shown that using modern control theory can aid in the exploration of a control methods that efficiently lowers virus propagation by increasing immunization. In addition, robust control is a crucial aspect that addresses the challenges of controlling the COVID-19 outbreak and improves upon previously proposed methods by considering for variations in system parameters. The H_∞ control is a widely used approach for robust control, and it is effective in tackling system uncertainty. However, it may not meet the desired transient response on its own. To address this, the model reference control can be used, which imposes the desired response on the closed-loop system. To counteract the effects of system nonlinearity, feedback linearization can be used to cancel its impact globally. Thus, developing a nonlinear robust control strategy is desirable in order to achieve better vaccination results.

This paper poses a novel approach for controlling the COVID-19 system via vaccination by addressing all the nonlinearity and uncertainty in the system, achieving satisfactory stability and performance, and utilizing the black hole optimization to improve the approach effectiveness. A modified SEIR model, having the characteristics of COVID-19, is used to formulate a dynamic model for the system. Then, the effectiveness of the proposed control method is assessed based on the national vaccination campaign of lombardy, Italy, as a case study.

The paper is organized as follows. Section 2 describes the methodologies of the study, including the mathematical representation of the COVID-19 system, the black hole optimization, and the control approach design. Section 3 presents the simulation results and their discussion, along with a comparison to previous works. Section 4 draws conclusion based on the results obtained.

2. Materials and methods

In this section, a mathematical model suitable for controlling the propagation of COVID-19 through vaccination is established using mathematical norms of epidemiology. The control strategy is then fully described, along with the methods and algorithms adopted to support the design of the control strategy.

2.1 Mathematical representation of COVID-19

The mathematical representation of the COVID-19 system is divided into two phases. The initial phase involves selecting an appropriate epidemic model, which is then modified by applying certain investigations and hypotheses to reflect the dynamic model of COVID-19 suited for vaccination control. The subsequent phase is to allocate the control input of vaccination in the chosen model. In this work, the following SEIR model is used for constructing the mathematical model of COVID-19 [10-12]:

$$\begin{aligned} \dot{S}(t) &= -\frac{\beta S(t) I(t)}{N} \\ \dot{E}(t) &= \frac{\beta S(t) I(t)}{N} - \epsilon E(t) \\ \dot{I}(t) &= \epsilon E(t) - \sigma I(t) \\ \dot{R}(t) &= \sigma I(t) \end{aligned} \tag{1}$$

where the variable N denotes the total population being studied, while the variables $S(t)$, $E(t)$, $I(t)$ and $R(t)$ represent the proportion of susceptible, exposed, infectious and immune individuals in the population at time t. The variables β, ϵ, and σ are the rate of virus infection over time, the reciprocal of the median latency timespan, and the reciprocal of the average infective period of the disease, respectively. The SEIR model splits the population depending on their disease status into: susceptible, exposed, infectious, and recovered (or immune) [2]:

$$N = S(t) + E(t) + I(t) + R(t) \tag{2}$$

Therefore, the population evolves over time as:

$$\dot{N} = \dot{S}(t) + \dot{E}(t) + \dot{I}(t) + \dot{R}(t) \tag{3}$$

To emulate the dynamical behavior of the COVID-19 outbreak, the following proposition are made:

Proposition 1: A worst-case scenario approach is adopted when studying the COVID-19 pandemic. Given the virus's highly contagious nature and the

prolonged healing time, it is reasonable to presume that the gross population is vulnerable, meaning that $S(t) = N$ [10].

Proposition 2: The death and birth rates are not considered significant because the risk of infection in neonates is considered negligible and the primary function of vaccination is to provide immunity and control, rather than treating an existing disease.

Proposition 3 With the advent of new rapid testing methods for the virus [16], delays in detecting and testing infected cases are no longer an issue, so the delays are neglected.

Proposition 1 results in that $S(t)/N = 1$. Using this value into Eq. (1) produces:

$$\begin{aligned} \dot{S}(t) &= -\beta I(t) \\ \dot{E}(t) &= \beta I(t) - \epsilon E(t) \\ \dot{I}(t) &= \epsilon E(t) - \sigma I(t) \\ \dot{R}(t) &= \sigma I(t) \end{aligned} \tag{4}$$

Furthermore, proposition 2 argues that the number of total people *N* remains constant [10, 12], hence:

$$\dot{E}(t) + \dot{I}(t) + \dot{R}(t) = -\dot{S}(t) \tag{5}$$

The equation above illustrates that the evolutions of $\dot{S}(t)$, $\dot{E}(t)$, $\dot{I}(t)$, and $\dot{R}(t)$ are interrelated. This fact can be used to simplify the model by concentrating on the states of immunity, exposure, and infection:

$$\begin{aligned} \dot{R}(t) &= \sigma I(t) \\ \dot{I}(t) &= \epsilon E(t) - \sigma I(t) \\ \dot{E}(t) &= \beta I(t) - \epsilon E(t) \end{aligned} \tag{6}$$

with $\dot{S}(t) = -\dot{R}(t) - \dot{I}(t) - \dot{E}(t)$. Proposition 3 declares that the amount of registered and tested instances of infection is equivalent ($I_t(t) = I_r(t)$). It is important to note that there may be a difference between the number of actual infected $I(t)$ and registered (tested positive) $I_r(t)$ cases because some individuals may have mild or no symptoms and thus may not be tested, but still able to spread the virus [10, 12]. Hence, a factor α is added to the model to transform it in terms of the official registered cases (the data used to develop the control strategy) [10]:

$$\alpha = \frac{I_r(t)}{I(t)} \tag{7}$$

Moreover, it is usually assumed that α maintains a consistent value for a specific country, however, it has been found to fluctuate significantly from one country to another. Research has revealed that the value of α varies from roughly 0.02 for Germany to 0.1 for Italy [10, 12]. It is important to take into account that α may not remain constant and may vary according to country when studying outcomes. Hence, it is accurate that:

$$\begin{aligned} R_r(t) &= \alpha R(t) \\ I_r(t) &= \alpha I(t) \\ E_r(t) &= \alpha E(t) \end{aligned} \tag{8}$$

Thus, Eq. (6) can be re-written as:

$$\begin{aligned} \dot{R}_r(t) &= \sigma I_r(t) \\ \dot{I}_r(t) &= \epsilon E_r(t) - \sigma I_r(t) \\ \dot{E}_r(t) &= \beta I_r(t) - \epsilon E_r(t) \end{aligned} \tag{9}$$

with $\dot{S}_r(t) = -\dot{R}_r(t) - \dot{I}_r(t) - \dot{E}_r(t)$. The primary goal of vaccination is to boost $R_r(t)$ and decrease $I_r(t)$, $S_r(t)$, and $E_r(t)$ which leads to a remarkable decrease in the transmission rate of the virus β. In this context, β can be recognized in relation to the vaccine control $u(t)$ as β is directly affected by vaccination [10]. Furthermore, the model's output $y(t)$ is selected to be the number of vaccinated (or immunized) individuals $R_r(t)$. Hence, the dynamics of the COVID-19 including vaccination control in state-space representation can be written as follows:

$$\begin{aligned} \dot{R}_r(t) &= \sigma I_r(t) \\ \dot{I}_r(t) &= \epsilon E_r(t) - \sigma I_r(t) \\ \dot{E}_r(t) &= \beta\big(u(t)\big) I_r(t) - \epsilon E_r(t) \\ y(t) &= R_r(t) \end{aligned} \tag{10}$$

and $\dot{S}_r(t) = -\dot{R}_r(t) - \dot{I}_r(t) - \dot{E}_r(t)$. The proposed control strategy addresses the fluctuation between the real and declared (tested) number of infectious individuals by considering the variables σ and ϵ to be unknown, with finite unknown bounds.

2.2 Black hole optimization (BHO) technique

BHO is a technique for solving optimization problems based on inspiration from the phenomenon of black holes. It is a metaheuristic population-based technique that begins by autonomously producing a group of solutions (candidates) and determining a specific optimization cost function for the problem at hand. These candidates are dispersed at random throughout the d-dimensional solution space, where d denotes the number of variables getting optimized.

Next, the cost of each candidate is calculated and the best (optimum) one, having the lowest cost value, is designated as the Black Hole (BH) while the other candidates are rated as regular stars. The algorithm is then updated based on the following convergence equation to guide the stars forward to the BH:

$$x_i(t+1) = x_i(t) + rand \times \left(x_{BH} - x_i(t)\right); \quad i \in \mathcal{R} = 1, 2, \dots, n \tag{11}$$

where $x_i(t+1)$ and $x_i(t)$ are the position of i-th star at iterations $(t+1)$ and (t), x_{BH} is the position of the BH, $rand$ is a real value that is generated randomly within the range of 0 to 1 inclusive, and n is the stars number. When a star achieves a lowest - cost placement than the current BH, it is identified as new BH. Then, the process of updating continues as the remaining stars come closer to the newfound BH. As the stars enter the range of the BH known as the event horizon, they are absorbed by the BH and replaced by a newer candidates supplied at random within the solution space. This replacement process ensures that the solution space is constantly updated, increasing the chance of finding the global optimum solution. The following relation is used to determine the event horizon radius with respect to the i-th star:

$$R = \frac{C_{BH}}{\sum_{i=1}^{N} C_i} \tag{12}$$

where C_{BH} and C_i are the BH and star cost indices, respectively. The BHO continues to be executed till the optimum values are realized after a certain batch of iterations [17-19].

BHO is a promising optimization technique that has several strong points over other optimization techniques. One of its primary strengths is faster convergence due to its ability to balance exploration and exploitation of the search space. It is also robust and less sensitive to noise, making it more reliable in finding optimal solutions. Also, it is capable of global optimization, making it suitable for a wide range of optimization problems. BHO has few parameters that require minimal tuning, making it easy to implement. Finally, BHO is flexible and can be applied to many optimization problems. Overall, BHO is a unique approach, combined with its global optimization capabilities, make it more efficient optimization technique for complex optimization problems [20].

2.3 Control approach design procedure

In this subsection, the proposed control method for COVID-19 is presented. The method uses the linearizing via feedback and the H_∞ paradigms to design a control law that can handle the nonlinearity and uncertainty inherent in the COVID-19 dynamic. Additionally, a model reference control is employed to achieve desired time response, where the features of a suitable reference model is designated as the baseline of the control system. The control law aims to provide robustness with proper tracking between the system states ($R_r(t)$, $I_r(t)$, and $E_r(t)$) and the reference states. Initially, the system model given in Eq. (10) shows that incompatible perturbations exist in the subsystem channels ($\dot{R}_r(t)$ and $\dot{I}_r(t)$), which cannot be handled by control without first rewriting the system equations into an analogous controllable form, in which the nonlinearity and uncertainty of the system are relaxed and located in the identical effect span as $\beta\big(u(t)\big)$. To achieve this, the ensuing state transformation is introduced [12, 18, 19, 21]:

$$z(t) = T\left(\begin{bmatrix} R_r(t) \\ I_r(t) \\ E_r(t) \end{bmatrix}\right) \in \mathcal{R}^3 \tag{13}$$

This mapping is executed in the following sequence:

$$\begin{aligned} z_1 &= R_r \\ z_2 &= \dot{z}_1 = \dot{R}_r \\ z_3 &= \dot{z}_2 = \ddot{z}_1 = \ddot{R}_r \end{aligned} \tag{14}$$

For simplicity, the time variable is omitted. Hence, the system model in terms of $z(t)$ becomes:

$$\begin{aligned} \dot{z}_1 &= z_2 \\ \dot{z}_2 &= z_3 \\ \dot{z}_3 &= -\epsilon\sigma z_2 - (\epsilon + \sigma) z_3 + \epsilon z_2 \beta(u) \\ y &= z_1 \end{aligned} \tag{15}$$

Alternatively, it can be formed in matrix notation as:

$$\begin{aligned} \dot{z} &= Az + Bz_2\beta(u) \\ y &= Cz \end{aligned} \tag{16}$$

with:

$$A = \begin{bmatrix} 0 & 1 & 0 \\ 0 & 0 & 1 \\ 0 & -\epsilon\sigma & -(\epsilon + \sigma) \end{bmatrix}, z = \begin{bmatrix} z_1 \\ z_2 \\ z_3 \end{bmatrix} \in \mathcal{R}^3,$$
$$B = \begin{bmatrix} 0 \\ 0 \\ \epsilon \end{bmatrix}, \text{and } C = [1 \quad 0 \quad 0] \tag{17}$$

It is important to emphasize that the initial stage of the proposed controller design strives to deal with the system's nonlinearity relying on linearization via feedback approach. This approach achieves accurate linearization, transforming the unknown nonlinear COVID-19 dynamical model into a complementary unknown linear description. The robust part is then designed to tackle the system's uncertainty [21]. As a consequence, the following is correct:

$$\beta(u) = \frac{1}{z_2}\beta_v(u) \in \mathcal{R} \tag{18}$$

where $\beta_v(u)$ is a supplementary virtual controller. Thus, incorporating Eq. (18) into Eq. (16) renders:

$$\begin{aligned} \dot{z} &= Az + B\beta_v(u) \\ y &= Cz \end{aligned} \tag{19}$$

where $A \in \mathcal{R}^{3\times3}$ and $B \in \mathcal{R}^3$ are uncertain due to the presence of the parametric uncertainty of ϵ and σ, which is indicated by variations in their actual values compared to their reported (nominal) values, due to the disparity between officially declared and real instances of contagion. Then, the robust section of the vaccination controller is synthesized based on the H_∞ control [21]. In this approach, the parametric uncertainties are excluded from the nominal part of the system and a tailored exogenous input is formed for them in the system model, as follows:

$$\epsilon = \epsilon_r + \delta_\epsilon \tag{20}$$

$$\sigma = \sigma_r + \delta_\sigma \tag{21}$$

where ϵ_r and σ_r are the nominal values and δ_ϵ, δ_σ are the uncertainties in the values of the parameters. Therefore, the system model becomes:

$$\begin{aligned} \dot{z} &= A_r z + B_1\delta_a(t,z,u) + B_r\beta_v(u) \\ y &= Cz \end{aligned} \tag{22}$$

where $\delta_a(t,z,u) = -\delta_{\epsilon\sigma}z_2 - \delta_{(\epsilon+\sigma)}z_3 + \delta_\epsilon\beta_v(u)$ denotes the system uncertainty, and:

$$A_r = \begin{bmatrix} 0 & 1 & 0 \\ 0 & 0 & 1 \\ 0 & -\epsilon_r\sigma_r & -(\epsilon_r+\sigma_r) \end{bmatrix}, \quad B_1 = \begin{bmatrix} 0 \\ 0 \\ 1 \end{bmatrix}, \quad \text{and} \quad B_r = \begin{bmatrix} 0 \\ 0 \\ \epsilon_r \end{bmatrix} \tag{23}$$

In this work, the reference model is chosen as [22]:

$$\begin{aligned} \dot{z}_d &= A_d z_d + B_d r \\ y_d &= C z_d \end{aligned} \tag{24}$$

with:

$$A_d = \begin{bmatrix} 0 & 1 & 0 \\ 0 & 0 & 1 \\ -\omega_n^3 & -2{,}15\omega_n^2 & -1{,}75\omega_n \end{bmatrix} \in \mathcal{R}^{3\times3}, \quad \text{and} \quad B_d = \begin{bmatrix} 0 \\ 0 \\ \omega_n^3 \end{bmatrix} \in \mathcal{R}^3 \tag{25}$$

where:

$z_d(t) \in \mathcal{R}^3$ is the reference model's state vector.
$r(t)$ is the input command of vaccination.
$y_d(t)$ is the reference model output.
ω_n is the natural frequency that is adjusted in order to create an appropriate time response.

The control law design for asymptotic tracking duty must comply with the criterion [18, 19, 21]:

$$\lim_{t\to\infty} \|e(t)\|_2 = 0 \tag{26}$$

where $e(t) \in \mathcal{R}^3$ represents the tracking error vector that is the deviation between the actual states of the system and the desired states of the reference model:

$$e = z - z_d \tag{27}$$

and:

$$\dot{e} = \dot{z} - \dot{z}_d \tag{28}$$

Putting Eqs. (22) and (24) into Eq. (28) yields:

$$\dot{e} = \begin{pmatrix} A_r z + \\ B_1\delta_a(t,e,u) + \\ B_r\beta_v(u) \end{pmatrix} - (A_d z_d + B_d r) \tag{29}$$

Adding/subtracting $A_r z_d$ to/from Eq. (29) gives:

$$\dot{e} = \begin{pmatrix} A_r e + \\ B_1\delta_a(t,e,u) + \\ B_r\beta_v(u) \end{pmatrix} + (A_r - A_d)z_d - B_d r \tag{30}$$

Now, let:

$$\beta_v(u) = \frac{1}{\epsilon_r}\left(\begin{matrix}\omega_n^3 r - \omega_n^3 z_{d1} + \\ \left(\epsilon_r\sigma_r - \right. \\ \left. 2.15\omega_n^2\right) z_{d2} + \\ \left(\left(\epsilon_r + \sigma_r\right) - \right. \\ \left. 1.75\omega_n\right) z_{d3}\end{matrix}\right) + \beta_R(u) \quad (31)$$

where $\beta_R(u)$ is the robust section of the controller that is used to boost the system's robustness. Then, the tracking error dynamics be as:

$$\begin{aligned} \dot{e} &= A_r e + B_1\delta_a(t,e,u) + B_r\beta_R(u) \\ h &= C_1 e + D_{12}\beta_R(u) \end{aligned} \quad (32)$$

where $h(t)$ denotes the vector of system outputs that are impacted by uncertainty. The magnitude of these outputs is controlled by using the weights defined in matrices C_1 and D_{12}. Essentially, the values in these matrices determine how much weight should be given to the elements of $h(t)$ in order to regulate the overall level of uncertainty in the system.

Proposition 4 [18, 19, 21]:

1) (A_r, B_1) and (A_r, B_r) are controllable.
2) (C_1, A_r) is observable.
3) $C_1^T D_{12} = \mathbf{0} \in \mathcal{R}^3$ and $D_{12}^T D_{12} = \varepsilon I \in \mathcal{R}^{3\times 3}$. where ε is a weight associated with $\beta_R(u)$.

The H_∞ control technique is used to develop controllers that are able to minimize the closed-loop impact of uncertainty by minimizing the H_∞ norm of the closed-loop transfer matrix $G_{h\delta}(s)$ between the uncertainty input $\delta_a(t,e,u)$ and the output $h(t)$ to achieve a value less than or equal to a specified threshold, denoted by γ [18, 19, 21]:

$$\|G_{h\delta}(s)\|_\infty \leq \gamma \quad (33)$$

where γ is a real positive number serves as an indicator of the system's robustness. This approach is used to ensure that the system remains stable and performs well in the existence of uncertainties. The state feedback controller $\beta_R(u)$ is used to adjust the system's behavior based on the error states and a gain matrix K_{β_R}. Hence [18, 19, 21]:

$$\beta_R(u) = K_{\beta_R} e; \text{ with } K_{\beta_R} = -\varepsilon^{-1} B_r^T P \quad (34)$$

with $P \in \mathcal{R}^{3\times 3}$ is a real symmetric positive definite matrix signifies the optimal and unique solution of the Riccati equation:

$$PA_r + A_r^T P - P\left[\begin{matrix}\varepsilon^{-1}B_r B_r^T - \\ \gamma^{-2}B_1 B_1^T\end{matrix}\right]P + C_1^T C_1 = 0 \quad (35)$$

The calculation of the Riccati equation is conducted based on the following Lyapunov function:

$$V(e) = e^T P e \quad (36)$$

This means that if the Riccati equation is solved, the stabilization of the COVID-19 system is ensured asymptotically in the sense of Lyapunov [23]. Thus, the complete vaccination-based control law be:

$$\beta(u) = \frac{1}{z_2}\left(\frac{1}{\epsilon_r}\left(\begin{matrix}\omega_n^3 r - \omega_n^3 z_{d1} + \\ \left(\epsilon_r\sigma_r - \right. \\ \left. 2.15\omega_n^2\right) z_{d2} + \\ \left(\left(\epsilon_r + \sigma_r\right) - \right. \\ \left. 1.75\omega_n\right) z_{d3}\end{matrix}\right) - \varepsilon^{-1}B_r^T P e\right) \quad (37)$$

The control approach proposed has the advantage of assuming that the variables ϵ and σ have known nominal values with unknown bounds. This means that the uncertainty input $\delta_a(t,e,u)$ is considered and analyzed in light of worst behavior [18, 19, 21]:

$$\delta_a(t,e,u) = K_\delta e; \text{ with } K_\delta = \gamma^{-2} B_1^T P \quad (38)$$

The BHO technique is used to determine the minimum value of γ that results in the minimization of $\|G_{h\delta}(s)\|_\infty$ as much as possible, along with the optimum value of ε and the optimum elements in the matrix C_1, using the following cost function for guiding this optimization process:

$$J_{BHO}(\gamma, \varepsilon, C_1) = \|G_{h\delta}(s)\|_\infty \quad (39)$$

In this sense, the design of the robust control section is approached in reverse by applying firstly the BHO algorithm. Then, the Riccati equation is solved, and the control law $\beta_R(u)$ is defined based on matrix P.

3. Results and discussion

This section evaluates the effectiveness of the proposed control approach to desirably control the COVID-19 epidemic by vaccination. The simulation results are analyzed and obtained with the aid of Matlab/Simulink for the following nominal values $\epsilon_r = \sigma_r = 0.2\, day^{-1}$ of the COVID-19 reports in the Italian province of Lombardy during the most

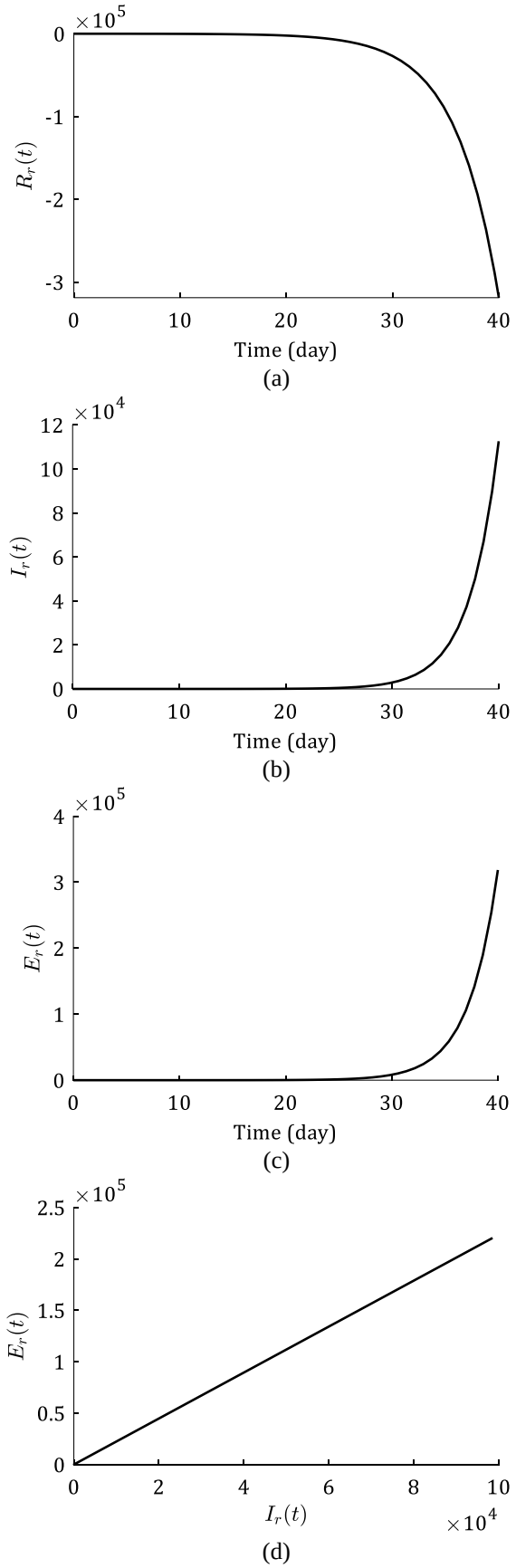

Figure. 1 Time responses of the open-loop COVID-19 system in terms of: (a) immune, (b) infectious, (c) exposed, and (d) exposed versus infectious individuals

severe stage of the virus spread, from February 23, 2020 to March 16, 2020 [24]. Firstly, Fig. 1 shows the responses of the open-loop COVID-19 system, which are depicted by the states of the immunized, infected, and exposed cases. The figure shows how the system is intrinsically unstable and how the infection swiftly dispersed, leading to a substantial rise in the count of persons who contract the disease. As a result, a trustworthy vaccination-based control approach is recommended to reduce the COVID-19 spread. The Italian ministry of health has adopted a policy for developing the vaccination campaign with the goal of ensuring immunity for a minimum of 70% of the total population of lombardy, with the target of vaccinating $6.6\ million$ individuals with a daily average of approximately 170 thousand people a day [25], leading to acquiring herd immunity [26], where two of every three individuals be immune, resulting in a gradual decrease of infection rates until they reach zero. The input signal of vaccination schedule is presented as shown in Fig. 2. In a subsequent step, the BHO is applied to assess the optimality of the control strategy. This algorithm is executed for (400) iterations based on Eq. (32) and the nominal values of the system parameters. The outcome of this evaluation are the optimal values for the parameters γ, ε, and C_1, which are summarized in Table 1. Then, the Riccati equation (expressed in Eq. (35)) is solved using the gained optimal values. Then, the solution matrix P, gain matrix K_{β_R}, and optimal cost are obtained as shown in Table 2. It is shown that the solution matrix P is positive definite and the cost value minimization has been effectively reduced below the minimum threshold γ. Hence, the robustness criterion of Eq. (33) has been satisfied, and the proposed control approach can realize better robustness for the COVID-19 system with closed-loop signals staying uniformly bounded. After that, the overall control law defined in Eq. (37), has been obtained for $\omega_n = 50\ rad/day$ and applied directly to the main model of the COVID-19 system outlined in Eq. (10), using all identified design parameters.

Fig. 3 displays the response of the COVID-19 control system in regards of nominal data, showing how the trajectory of vaccinated people desirably follows the reference response and input signal, and the number of vaccinated individuals has increased as a result of vaccination, leading to a decrease in the number of infectious and exposed individuals (shown in Fig. 4), as anticipated given the rise in immunization. Thus, despite the nonlinear nature of COVID-19, the closed-loop system gained adequate stabilization and performancenominal data.

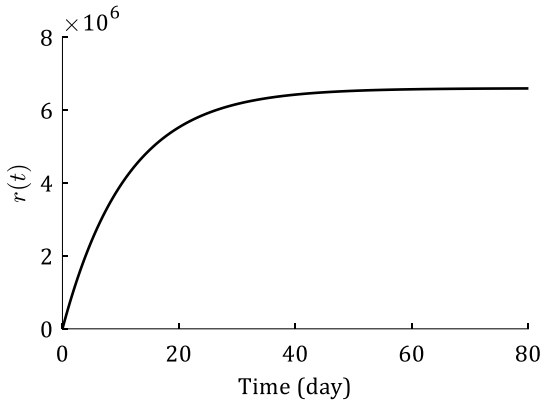

Figure. 2 Input signal of the vaccination schedule

Table 1. Optimal values of the design optimized parameters

Optimized Parameter	Optimal Value
γ	0,6207
ε	0,0050
C_1	$\begin{bmatrix} 3{,}0381 & 7{,}2204 & 7{,}1474 \\ 4{,}3491 & 7{,}9234 & 6{,}2379 \\ 5{,}9375 & 4{,}3601 & 3{,}5643 \\ 0 & 0 & 0 \end{bmatrix}$

Table 2. Values of the solution matrix P, gain matrix K_{β_R}, and optimal cost

P, K_{β_R}, and Optimal cost	Value
P	$\begin{bmatrix} 19.6009 & 14.9047 & 3.4250 \\ 14.9047 & 16.4561 & 5.4968 \\ 3.4250 & 5.4968 & 4.5132 \end{bmatrix}$
K_{β_R}	$[-137.0017 \quad -219.8729 \quad -180.5295]$
$\|G_{h\delta}(s)\|_\infty$	0.4607

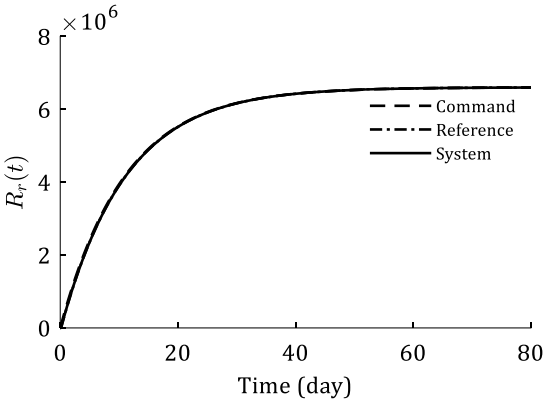

Figure. 3 Vaccinated people trajectories (response) in regards of nominal data

Fig. 5 shows that the deviation (or tracking error) between the system and reference model states tends to zero as time progresses, which

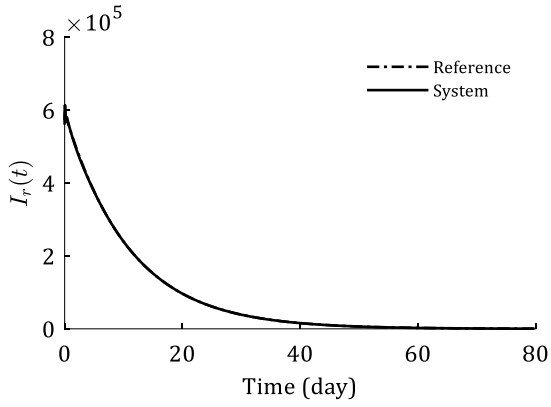

(a)

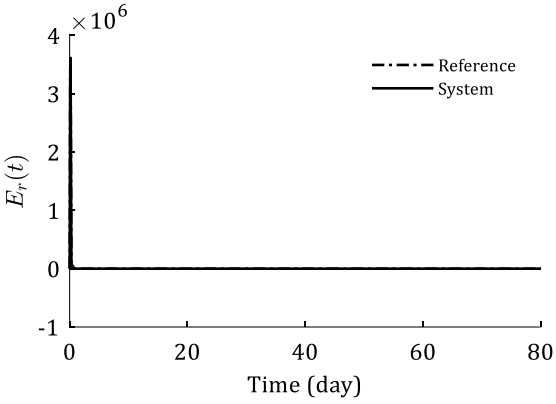

(b)

Figure. 4 Trajectories of the: (a) infectious $I_r(t)$ and (b) exposed $E_r(t)$ states of the nominal closed-loop system

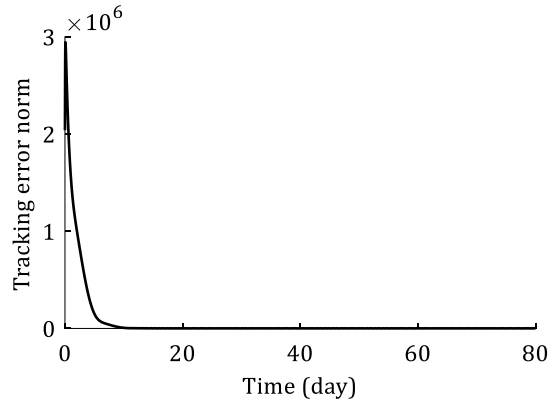

Figure. 5 Tracking error norm of the closed-loop system

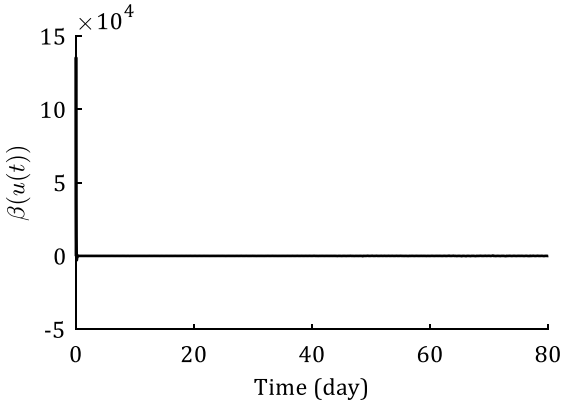

Figure. 6 Activity of the control action

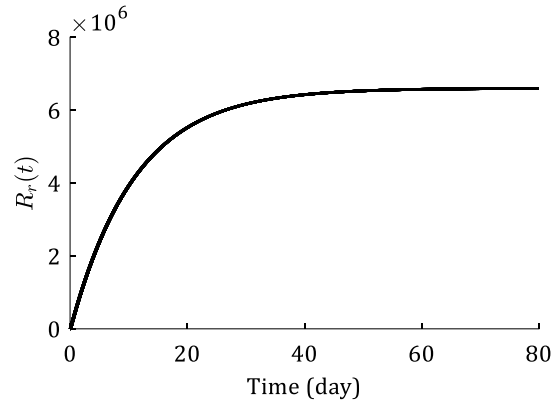

(a)

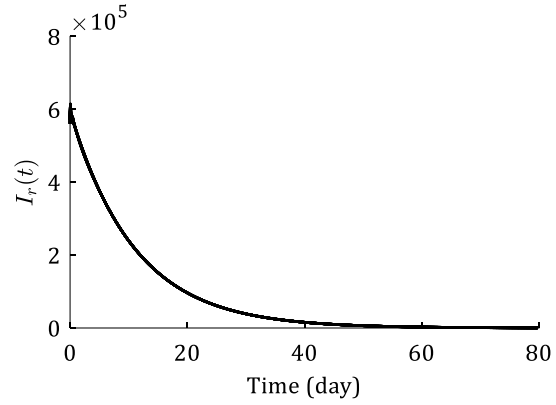

(b)

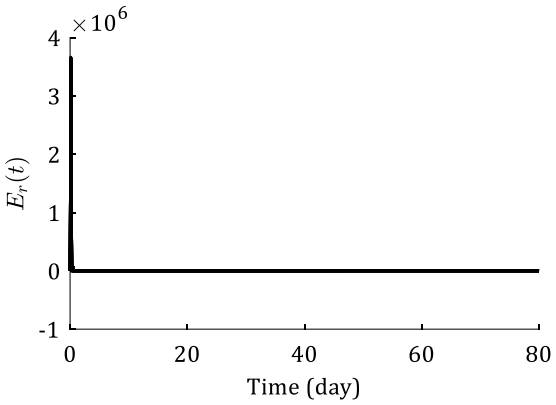

(c)

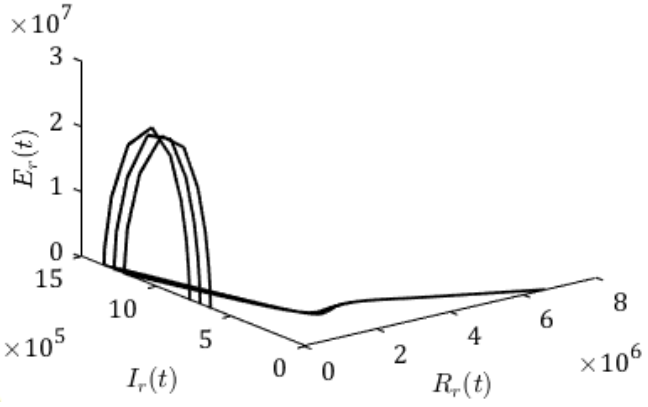

(d)

Figure. 7 State dynamics of the COVID-19 control system under all variations: (a) immune, (b) infectious, (c) exposed, and (d) combined

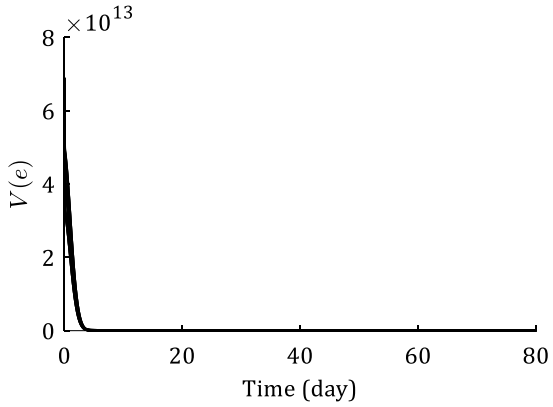

Figure. 8 The Lyapunov function conduct under all variations

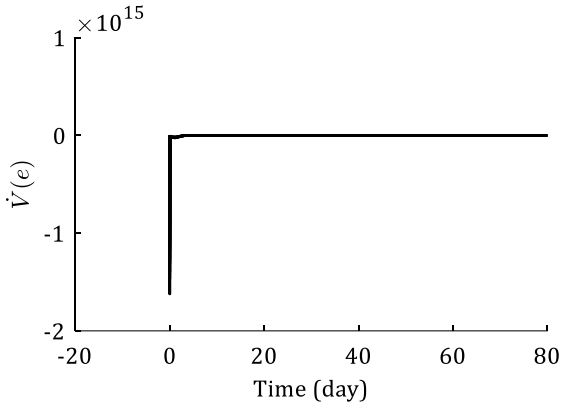

Figure. 9 Properties of $\dot{V}(e)$

confirms that the tracking property specified in Eq. (26) has been achieved. The role of the vaccination control input is visualized in Fig. 6, where it can be illustrated that the control action is effectively proportioned given the large number of the vaccinated individuals.

Earlier it has been previously stated that a factor α is introduced to address the issue that arose as a result of the difference between real and registered disease cases, and it is assessed to be 0.1 for the Italian people. Thus, to study the effectiveness of the proposed control plan, variations of $\pm 10\%$ from the declared (nominal) values of the variables ϵ and σ are taken into account. As a corollary of this, Fig. 7 shows the state dynamics of the variated COVID-19 closed-loop system, proving that the system under control remains robust and stable with reasonable performance despite perturbations and nonlinearity.

The stability criterion of the equilibrium point ($e = \mathbf{0} \in \mathcal{R}^3$) is analyzed in Figs. 8 and 9 based on the sense of the Lyapunov theory. These figures show that the Lyapunov function is positive definite ($V(e) > 0$ for all $e \in \mathcal{R}^3$) and its time derivative is negative definite ($\dot{V}(e) < 0$ for all $e \in \mathcal{R}^3$), which indicates that the point is asymptotically stable.

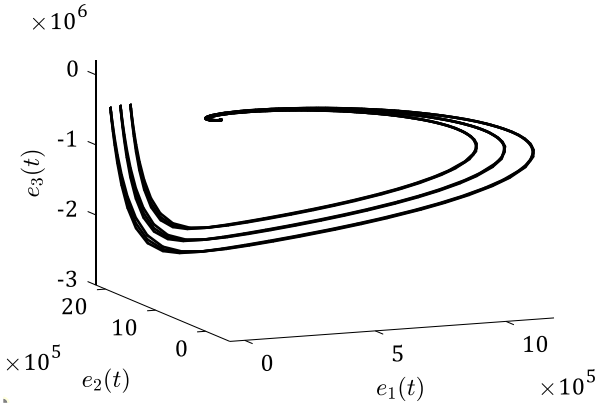

Figure 10. Phase plane analysis of the error states

Furthermore, the Lyapunov function candidate as given in Eq. (36) is radially unbounded, i.e., $V(e) \to \infty$ as $\|e\|_2 \to \infty$, ensuring the global asymptotic stability even under system perturbations.

The phase plane plot of the tracking error states after control is shown in Fig. 10. It can be observed that the error vector ($e \in \mathcal{R}^3$) converges to zero for all variations in the system parameters. Thus, the control system exhibited global asymptotic tracking, towards the steady-state point ($R_r(\infty) = 6.6 \times 10^6$, $I_r(\infty) = 0$, $E_r(\infty) = 0$), as illustrated also in Fig. 7.

The previously described findings illustrate that the proposed control law was efficient in controlling the COVID-19 pandemic by the use of vaccination. The control strategy has managed to decrease the rate of virus transmission within a proper amount of time. The control law was able to implement the vaccination plan with an effective and satisfactory control action, exhibiting desirable nominal stability and robustness characteristics for the COVID-19 system. The control approach effectively mitigated perturbations with high robustness, and achieved desirable time responses by closely following the necessary specs provided by the reference model. It is crucial to ensure that all the considered values of γ should always satisfy the essential inequality:

$$\varepsilon^{-1} B_r B_r^T - \gamma^{-2} B_1 B_1^T \geq \mathbf{0} \in \mathcal{R}^3 \quad (40)$$

If not, the Riccati equation cannot be solved or it might not possess positive definiteness and the control approach might be deemed unsuccessful.

The proposed control method, as well as the previously posed approaches, provided solutions to COVID-19 guided by control engineering theories, through the adoption of specific tactics and policies in government decision-making relying on accurate analyses that estimate proper outcomes if these methodologies are properly implemented. However, the proposed approach has achieved better results by managing the vaccination process as a means of controlling the pandemic, which differs from the previous methods that relied solely on implementing quarantine policies [10-15]. Also, the mathematical model proposed here has depicted the sufficient and impactful states of pandemic, offering a satisfactory simulation of the COVID-19 system. This approach is distinct from previous methods, where the system models were formed with either exaggerated states, as in [11, 13-15, 24], making the control method less feasible, or with poor states, as in [10, 12], that may fail to accurately reflect the pandemic behavior.

Furthermore, the performance of the proposed controller was significantly superior to those of the previous works that were presented in [12, 24]. In [12], a robust nonlinear control law for COVID-19 has been posed. However, the method exhibited notable drawback compared to the current proposed work. The controller has exhibited discontinuous characteristics due to the sign operator $sgn(.)$ that lead the system signals to chatter noisily with a control action of (12×10^6 and 8×10^6) at the start of the response, which is regarded a very high amount regarding to the greatest value of output, which was approximately 4500 individuals to be saved by quarantine. In contrast, the proposed control law had continuous features resulting in smooth signals with an adequate starting control action comparing to the high value of the vaccinated people, As shown in Fig. 6. In [24], a vaccination control strategy was presented using metric temporal logic for the same study period and data. However, the number of immune individuals in this method reached the value of $6.6\ million$ after $49\ days$ form the start of vaccination response, while the proposed controller has achieved the required immunity after about $25\ days$ with no overshoot and unwanted behaviors. Besides, the infectious and exposed actions are considered with zero initial conditions, which is not actually accepted for the COVID-19 system. On the other hand, the proposed technique started to compensate the system with initial conditions of 6×10^5 and 3.6×10^6 for infectious and exposed trajectories, respectively. In [24], the vaccination control was assigned as an external input in the mathematical model. In this case, the derived model of the system may suffer from the singularity issue. In a certain time, the system dynamics will be equal with opposite signs, leading to cancel each other. Consequently, dealing with the vaccination control as an argument of the parameter β in this work was more practical convincing action.

4. Conclusion

In this work, a new powerful control algorithm

was proposed for COVID-19 through vaccination based on feedback linearization and H_∞ control to tackle the system perturbations (nonlinearities and uncertainties). An adequate mathematical model for COVID-19 has been formulated depending on the SEIR epidemiological model and COVID-19 specs, where the system variables were regarded as having constrained variation and being unknown. Besides, optimal control was achieved by compensating for worst action of uncertainties and using the BHO technique for parameter optimization. The results have demonstrated successful control for COVID-19 through vaccination in Lombardy in a short length of time with increased stability and performance, allowing to proclaim the region as a safe (or white) zone. Finally, future research might include the use of the proposed control method to additional regions or it may include adding extra classes of population to handle more complexity with high precision.

Conflicts of interest

The authors declare no conflict of interest.

Author contributions

Conceptualization, A. H. Mhmood, H. I. Ali, A. B, Rakan; methodology, A. H. Mhmood, H. I. Ali, H. A. Mohammed; software, A. H. Mhmood, M. R. Subhi, Y. Kh. Yaseen; formal analysis, A. H. Mhmood, H. I. Ali; investigation, A. H. Mhmood, M. R. Subhi, Y. Kh. Yaseen; writing—original draft, A. H. Mhmood, A. B. Rakan; writing—review and editing, A. H. Mhmood; supervision, H. I. Ali.

Notation list

Notation	Description
N	Study total population
$S(t)$, $E(t)$, $I(t)$ and $R(t)$	State variables of susceptible, exposed, infectious and immune individuals
β	Rate of virus infection
ϵ	Reciprocal of the median latency timespan
σ	Reciprocal of the disease average infective period
α	Factor of transformation from actual to reported data
$R_r(t)$, $I_r(t)$, and $E_r(t)$	State variables of immune, exposed, and infectious individuals in terms of reported data
d	Number of the optimized variables
$x_i(t+1)$ and $x_i(t)$	Positions of i-th star at iterations $(t+1)$ and (t),
x_{BH}	Position of the black hole
$rand$	Random number between 0 and 1
n	Stars of the black hole method
C_{BH} and C_i	Costs of the black hole and i-th star
$z(t)$	New state vector of the system
$\mathcal{R}^3$	Three-dimensional space
$T(.)$	Operator of the diffeomorphism mapping
$\beta(u)$	Control function
A, B, and C	System matrices
$\beta_v(u)$	Supplementary virtual controller
ϵ_r and σ_r	Nominal values of ϵ *and* σ
δ_ϵ and δ_σ	Uncertainties of ϵ *and* σ
δ_a	Overall system uncertainty
z_d	State vector of the reference model
A_d, B_d, and C_d	Matrices of the reference model
ω_n	Natural frequency
$r(t)$	Input command of vaccination
$e(t)$	Tracking error vector
$\beta_R(u)$	Robust section of the controller
$h(t)$	Vector of system outputs impacted by uncertainty
C_1 and D_{12}	Weighting matrices
ε	Weight associated with $\beta_R(u)$
$G_{h\delta}(s)$	closed-loop transfer matrix between $\delta_a(t,e,u)$ and $h(t)$
γ	Robustness indicator
K_{β_R}	Gain matrix of $\beta_R(u)$
K_δ	Gain matrix of $\delta_a(t,e,u)$
P	Solution matrix of the Riccati equation
$V(e)$	Lyapunov function
$\|.\|_\infty$	Infinity norm
$J_{BHO}(.)$	Cost function of BHO

References

[1] W. H. Organization. (2020). Coronavirus disease (COVID-19) situation reports. Available: https://www.who.int/emergencies/diseases/novel-coronavirus-2019/situation-reports.

[2] H. A. Rad and A. Badi, "A study on control of novel corona-virus (2019- nCoV) disease process by using PID controller", *MedRxiv*, 2020.

[3] P. Yang, J. Qi, S. Zhang, X. Wang, G. Bi, Y. Yang, B. Sheng, and G. Yang, "Feasibility study of mitigation and suppression strategies for controlling COVID-19 outbreaks in London and Wuhan", *PLOS ONE*, Vol. 15, No. 8, p. e0236857, 2020.

[4] H. Sjödin, A. F. Johansson, Å. Brännström, Z. Farooq, H. K. Kriit, A. W. Smith, C. Åström, J. Thunberg, M. Söderquist, and J. Rocklöv, "COVID-19 healthcare demand and mortality in Sweden in response to non-pharmaceutical mitigation and suppression scenarios",

International Journal of Epidemiology, Vol. 49, No. 5, pp. 1443-1453, 2020.

[5] J. S. Weitz, S. J. Beckett, A. R. Coenen, D. Demory, M. D. Mirazo, J. Dushoff, C. Y. Leung, G. Li, A. Măgălie, and S. W. Park, "Modeling shield immunity to reduce COVID-19 epidemic spread", *Nature Medicine*, Vol. 26, No. 6, pp. 849-854, 2020.

[6] O. A. Hammad, H. Alduraidi, S. A. Hammad, A. Alnazzawi, H. Babkair, A. A. Hammad, I. Nourwali, F. Qasem, and N. D. Odeh, "Side Effects Reported by Jordanian Healthcare Workers Who Received COVID-19 Vaccines", *Vaccines*, Vol. 9, No. 6, p. 577, 2021.

[7] R. V. Barnabas and A. Wald, "A Public Health COVID-19 Vaccination Strategy to Maximize the Health Gains for Every Single Vaccine Dose", *Annals of Internal Medicine*, Vol. 174, No. 4, pp. 552-553, 2021.

[8] L. J. De Picker, M. C. Dias, M. E. Benros, B. Vai, I. Branchi, F. Benedetti, A. Borsini, J. C. Leza, H. Kärkkäinen, M. Männikkö, C. M. Pariante, E. S. Güngör, A. Szczegielniak, R. Tamouza, A. V. Markt, P. F. Poli, J. Beezhold, and M. Leboyer, "Severe mental illness and European COVID-19 vaccination strategies", *The Lancet Psychiatry*, Vol. 8, No. 5, pp. 356-359, 2021.

[9] V. M. Kumar, S. R. P. Perumal, I. Trakht, and S. P. Thyagarajan, "Strategy for COVID-19 vaccination in India: the country with thesecond highest population and number of cases", *npj Vaccines*, Vol. 6, No. 1, p. 60, 2021.

[10] F. Casella, "Can the COVID-19 Epidemic Be Controlled on the Basis of Daily Test Reports?", *IEEE Control Systems Letters*, Vol. 5, No. 3, pp. 1079-1084, 2021.

[11] G. Rohith and K. B. Devika, "Dynamics and control of COVID-19 pandemic with nonlinear incidence rates", *Nonlinear Dynamics*, Vol. 101, No. 3, pp. 2013-2026, 2020.

[12] M. A. Hadi and H. I. Ali, "Control of COVID-19 system using a novel nonlinear robust control algorithm", *Biomedical Signal Processing and Control*, Vol. 64, p. 102317, 2021.

[13] J. Köhler, L. Schwenkel, A. Koch, J. Berberich, P. Pauli, and F. Allgöwer, "Robust and optimal predictive control of the COVID-19 outbreak", *Annual Reviews in Control*, Vol. 51, pp. 525-539, 2021.

[14] A. Rajaei, M. Raeiszadeh, V. Azimi, and M. Sharifi, "State estimation-based control of COVID-19 epidemic before and after vaccine development", *Journal of Process Control*, Vol. 102, pp. 1-14, 2021.

[15] B. Cao and T. Kang, "Nonlinear adaptive control of COVID-19 with media campaigns and treatment", *Biochemical and Biophysical Research Communications*, Vol. 555, pp. 202-209, 2021.

[16] F. Colavita, F. Vairo, S. Meschi, M. B. Valli, E. Lalle, C. Castilletti, D. Fusco, G. Spiga, P. Bartoletti, S. Ursino, M. Sanguinetti, A. Di Caro, F. Vaia, G. Ippolito, and M. R. Capobianchi, "COVID-19 Rapid Antigen Test as Screening Strategy at Points of Entry: Experience in Lazio Region, Central Italy, August–October 2020", *Biomolecules*, Vol. 11, No. 3, p. 425, 2021.

[17] H. Deeb, A. Sarangi, D. Mishra, and S. K. Sarangi, "Improved Black Hole optimization algorithm for data clustering", *Journal of King Saud University - Computer and Information Sciences*, Vol. 34, No. 8, Part A, pp. 5020-5029, 2022.

[18] A. H. Mhmood and H. I. Ali, "Optimal H-infinity Integral Dynamic State Feedback Model Reference Controller Design for Nonlinear Systems", *Arabian Journal for Science and Engineering*, Vol. 46, No. 10, pp. 10171-10184, 2021.

[19] A. H. Mhmood and H. I. Ali, "Optimal adaptive guaranteed-cost H-infinity model reference controller design for nonlinear systems", *International Journal of Dynamics and Control*, Vol. 10, No. 3, pp. 843-856, 2022.

[20] L. Abualigah, M. A. Elaziz, P. Sumari, A. M. Khasawneh, M. Alshinwan, S. Mirjalili, M. Shehab, H. Y. Abuaddous, and A. H. Gandomi, "Black hole algorithm: A comprehensive survey", *Applied Intelligence*, Vol. 52, No. 10, pp. 11892-11915, 2022.

[21] H. I. Ali and A. H. Mhmood, "Nonlinear H-Infinity Model Reference Controller Design", *International Review of Automatic Control (IREACO)*, Vol. 14, No. 1, pp. 39-50, 2021.

[22] R. S. Gopi, S. Srinivasan, K. Panneerselvam, Y. Teekaraman, R. Kuppusamy, and S. Urooj, "Enhanced Model Reference Adaptive Control Scheme for Tracking Control of Magnetic Levitation System", *Energies*, Vol. 14, No. 5, p. 1455, 2021.

[23] Y. D. Mfoumboulou and M. E. S. Mnguni, "Development of a new linearizing controller using Lyapunov stability theory and model reference control", *Indonesian Journal of Electrical Engineering and Computer Science*, Vol. 25, No. 3, pp. 1328-1343, 2022.

[24] Z. Xu, B. Wu, and U. Topcu, "Control strategies for COVID-19 epidemic with vaccination, shield immunity and quarantine: A metric temporal logic approach", *PLOS ONE*, Vol. 16, No. 3, p. e0247660, 2021.

[25] G. Giacopelli, "A Full-Scale Agent-Based Model to Hypothetically Explore the Impact of Lockdown, Social Distancing, and Vaccination During the COVID-19 Pandemic in Lombardy, Italy: Model Development", *JMIRx Med*, Vol. 2, No. 3, p. e24630, 2021.

[26] C. R. MacIntyre, V. Costantino, and M. Trent, "Modelling of COVID-19 vaccination strategies and herd immunity, in scenarios of limited and full vaccine supply in NSW, Australia", *Vaccine*, Vol. 40, No. 17, pp. 2506-2513, 2022.